Capacity Density Optimization by Fractional Frequency Partitioning

Martin Taranetz, Josep Colom Ikuno, Markus Rupp

Vienna University of Technology, Institute of Telecommunications
Gusshausstrasse 25/389, A-1040 Vienna, Austria
Email: {mtaranet, jcolom, mrupp}@nt.tuwien.ac.at

***Abstract*—This paper presents a fractional frequency reuse optimization scheme based on capacity density. It assigns a given user to the frequency subband with maximum achievable capacity density $(\mathrm{bit/s/m^2})$. We formulate the optimization problem and solve it by simulation. Unlike in previous work, the problem is solved assuming interference limitation in all subbands. A sectorized layout with three-dimensional antenna radiation patterns is utilized, which includes the effect of antenna downtilting on the signal-to-interference-plus-noise ratio distribution. The simulation results show that the proposed scheme outperforms conventional Reuse-1- and Reuse-3 schemes in terms of average- and cell-edge performance.**

***Index Terms*—Fractional Frequency Reuse, Co-Channel Interference Mitigation, Reuse-Partitioning, Capacity Density.**

I. Introduction

Downlink throughput performance in cellular systems is mainly limited by Inter-cell Interference (ICI). Traditionally, ICI is handled by classical clustering techniques, of which a cellular network using a Frequency Reuse Factor of 3 ($\mathrm{FRF_3}$) would be an example. While these Co-Channel Interference (CCI) mitigation techniques reduce interference, which is especially crictical for users at the cell edge, they compromise system throughput due to the resource partitioning [1–8].

In order to balance the cell-edge throughput and the overall throughput, Fractional Frequency Reuse (FFR) has been proposed [9–12]. This reuse partitioning scheme combines the benefits of low and high Frequency Reuse Factors (FRFs) by dividing the cell in two zones: center and edge. The total available bandwidth B_{TOT} is split into a center band B_{FR} and an edge band B_{PR}. While the center band is reused with a low reuse factor by all users in the center zones, thus denominated Full Reuse (FR) zones, the edge band, assigned to the Partial Reuse (PR) zones, utilizes a higher order reuse scheme in order to better serve edge users. As common in literature [2–5, 10–13], $\mathrm{FRF_1}$ is used for the FR zones, while the PR zones employ $\mathrm{FRF_3}$.

Unlike in previous work [12, 14], interference limitation is assumed in the PR zones. So, the Signal-to-Interference-plus-Noise Ratio (SINR) in this zones is not reduced to an Signal-to-Noise Ratio (SNR), which directly impacts the achievable performance of the partitioning scheme. The commonly found flat scenario [1, 11–14] is extended by taking transmitter- and receiver height and Three-dimensional (3-D) antenna radiation patterns into account. This system model allows the investigation on the impact of antenna tilting on the systems achievable performance.

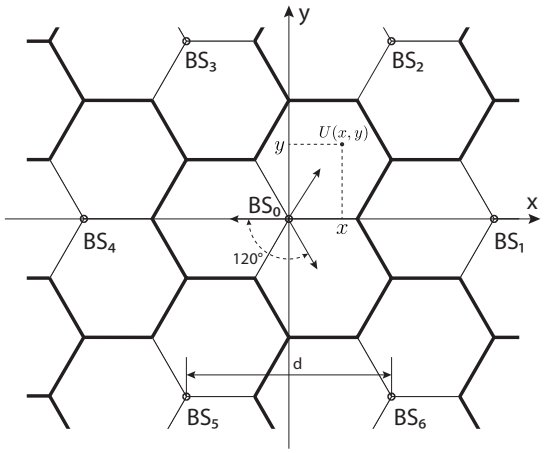

Fig. 1: Cellular system with hexagonal sectors. Sites are separated by a distance d, each holding three sectors separated $120°$. $U(x, y)$ shows a user positioned at (x, y).

Although throughput is the practical measure, we used channel capacity [15] as a theoretical upper bound and as performance metric which allows for more convenient mathematical expressions.

Overall capacity does not provide information about the single users' performance. Therefore, the achievable per-user capacity $(\mathrm{bit/s/User})$ is investigated. For its analysis, the concept of per-area capacity $(\mathrm{bit/s/Unit\ of\ Surface})$, also termed *capacity density* will be introduced. With the assumption of constant user density, both concepts are equivalent[1]. It is therefore analogously used to the per-user performance throughout this paper.

FFR optimization in this work is aimed at maximizing the average capacity density $\bar{c}$, while satisfying a minimum required $c_{5\%}$ cell-edge performance (analogous to the concept of ensuring a minimum edge user throughput) and minimizing the $c_{95\%}$ peak performance loss (analogous to the peak user throughput).

After introducing the system model in Section II, the target of this work is translated into an optimization problem in

[1] see Section III-D

Section III. Section IV proposes an optimal solution, which is verified in Section V by simulations in a 3-D sectorized scenario. We conclude the paper in Section VI.

II. System Model

For the system model, a hexagonal grid layout of cells, each consisting of three regularly shaped sectors, as shown in Figure 1, is utilized. Each site is equipped with three directional antennas, spaced out 120°.

In this paper, the channel power gain between two points separated by a distance r is restricted to the path loss. To model the macroscopic path loss, an exponential path loss model is used [16], expressed as $L(r)|_{\mathrm{dB}} = 20\log_{10}(\mathrm{c}_0/(4\pi f_\mathrm{c})) - \alpha 10\log_{10}(r)$, where α is the path loss exponent, c_0 denotes the speed of light and f_c is the center frequency.
Let $G_{\mathrm{Tx}}(x,y)|_{\mathrm{dB}}$ denote the additional power gain of a directional antenna at position (x,y). Then, assuming that BS_0 is located at the coordinate origin, the received power density $p_{\mathrm{Rx}}(x,y)$ (dBm/Hz) is expressed as

$$p_{\mathrm{Rx}}(x,y)|_{\frac{\mathrm{dBm}}{\mathrm{Hz}}} = p_{\mathrm{Tx}}|_{\frac{\mathrm{dBm}}{\mathrm{Hz}}} + G_{\mathrm{Tx}}(x,y)|_{\mathrm{dB}} + L\left(\sqrt{x^2+y^2}\right)|_{\mathrm{dB}}, \tag{1}$$

where $p_{\mathrm{Tx}}|_{\frac{\mathrm{dBm}}{\mathrm{Hz}}}$ is the transmit power density and the antenna gain $G_{\mathrm{Tx}}(x,y)|_{\mathrm{dB}}$ is obtained from the radiation pattern of the antenna.

III. Reuse-Partitioning Optimization

Typically, ICI mitigation techniques are confronted with the problem that enhanced cell-edge performance is traded off against overall system throughput [1, 2, 11, 14, 17, 18]. Optimization of ICI mitigation schemes aims at maximizing overall throughput while maintaining a minimum performance at cell-edge and minimizing peak performance loss. However, overall throughput does not provide information about the performance of the single users. Therefore, optimization in this paper aims at maximizing the average per-user throughput, which is represented by the concept of capacity density, as displayed in Section III-D.

A. Optimization Problem

An FFR partitioning scheme splits the cell and the total available bandwidth B_{TOT} in two parts: center and edge. As shown in Figure 2, FFR completely isolates the center- and cell-edge frequency bands. Therefore, $B_{\mathrm{TOT}} = B_{\mathrm{FR}} + 3B_{\mathrm{PR}}$, where B_{FR} and B_{PR} denote the FR- and PR bandwidths respectively. The normalized FR bandwidth β_{FR} is defined as $\beta_{\mathrm{FR}} = B_{\mathrm{FR}}/B_{\mathrm{TOT}}$, with $\beta_{\mathrm{FR}} \in [0,1]$. The FR- and PR zones are separated by the partitioning boundary ρ (see Figure 2). The FFR partitioning scheme is then parametrized by the pair $(\rho, \beta_{\mathrm{FR}})$.

The aim is to find the optimal pair[2] $(\rho^*, \beta^*_{\mathrm{FR}})$ to maximize per-user performance while achieving a minimum performance at cell edge and minimum peak-performance loss. Thus, the problem can be formulated as

$$\begin{aligned} \max \quad & \bar{c}\,(\rho, \beta_{\mathrm{FR}}) \\ \text{subject to} \quad & 0 \le \beta_{\mathrm{FR}} \le 1 \\ & \rho \in \mathcal{A}_{\mathrm{cell}} \\ & c_{5\%} \ge \mathrm{c}_1 \\ & c_{95\%} \ge \mathrm{c}_2, \end{aligned} \tag{2}$$

where the first two constraints represent the FFR scheme and the last two the cell-edge ($c_{5\%}$) and peak ($c_{95\%}$) constraints (c_1, c_2), respectively. The average capacity density $\bar{c}\,(\rho, \beta_{\mathrm{FR}})$ as a measure for the average per-user throughput is defined in Section III-D. The term $\mathcal{A}_{\mathrm{sector}}$ denotes the corresponding sector region.

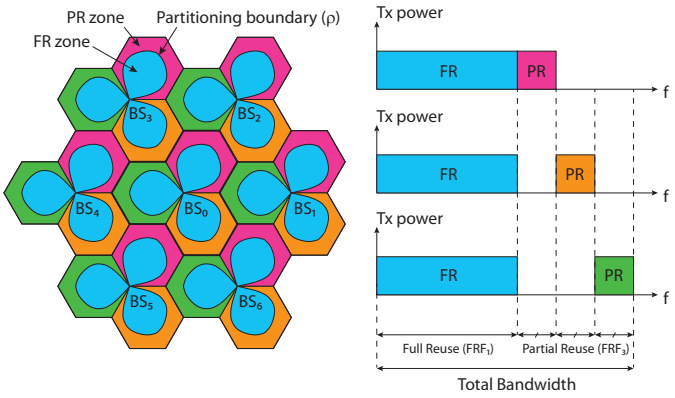

Fig. 2: FFR scheme using FRF_3: Cell cluster (left) and bandwidth partitioning (right).

B. Bandwidth Density and Capacity Density

Considering a uniform probability distribution of the users over the cell, varying the partitioning boundary ρ effectively alters the amount of physical resources that can be allocated to each user. As a zone (FR or PR) increases in size, so decreases the amount of resources per user on it. To take this into account in the analysis, a normalized *bandwidth density* $b_{\rho,\beta_{\mathrm{FR}}}(x,y)$ (Hz/Unit of Surface) is defined as

$$b_{\rho,\beta_{\mathrm{FR}}}(x,y) = \begin{cases} \frac{\beta_{\mathrm{FR}}}{A_{\mathrm{FR}}(\rho)}, & (x,y) \in \text{FR zone} \\ \frac{\frac{1}{3}(1-\beta_{\mathrm{FR}})}{A_{\mathrm{PR}}(\rho)}, & (x,y) \in \text{PR zone}, \end{cases} \tag{3}$$

with $A_{\mathrm{FR}}(\rho)$ and $A_{\mathrm{PR}}(\rho)$ denoting the area of the FR- and PR zones, respectively. A user at position (x,y) then achieves a *capacity density* (per-area capacity (bit/s/Unit of Surface)):

$$c_{\rho,\beta_{\mathrm{FR}}}(x,y) = b_{\rho,\beta_{\mathrm{FR}}}(x,y)\log_2\left(1+\gamma_\rho(x,y)\right), \tag{4}$$

where $\gamma_\rho(x,y)$ denotes the SINR at position (x,y). With

$$\gamma_\rho(x,y) = \begin{cases} \mathrm{SINR}_{\mathrm{FR}}(x,y), & (x,y) \in \text{FR zone} \\ \mathrm{SINR}_{\mathrm{PR}}(x,y), & (x,y) \in \text{PR zone}, \end{cases} \tag{5}$$

[2]The symbol * indicates optimal values in terms of the optimization problem

for a given partitioning boundary (ρ), (4) can be rewritten as:

$$c_{\rho,\beta_{\mathrm{FR}}}(x,y) = \begin{cases} c_{\mathrm{FR},\rho,\beta_{\mathrm{FR}}}(x,y), & (x,y) \in \text{FR zone} \\ c_{\mathrm{PR},\rho,\beta_{\mathrm{PR}}}(x,y), & (x,y) \in \text{PR zone}, \end{cases} \tag{6}$$

where

$$c_{\mathrm{FR},\rho,\beta_{\mathrm{FR}}}(x,y) = \frac{\beta_{\mathrm{FR}}}{A_{\mathrm{FR}}(\rho)} \log_2\left(1 + \mathrm{SINR}_{\mathrm{FR}}(x,y)\right), \tag{7}$$

$$c_{\mathrm{PR},\rho,\beta_{\mathrm{FR}}}(x,y) = \frac{\frac{1}{3}(1-\beta_{\mathrm{FR}})}{A_{\mathrm{PR}}(\rho)} \log_2\left(1 + \mathrm{SINR}_{\mathrm{PR}}(x,y)\right). \tag{8}$$

C. User Distribution

A user located at (x, y) is either assigned to the FR- or PR zone. The zones differ in allocated bandwidth and experienced SINR (see Figure 2). Thus, the position of the users influences the optimal bandwidth allocation and whether a user should be allocated to the FR- or PR zone.

The user distribution is described by a user-density function $u(x, y)$ (Users/Unit of Surface). In this paper, the user density is assumed to be constant, i.e., $u(x, y) = u$.

D. Definition of Average Capacity Density

As a performance metric for the optimization target, the *average capacity density* (bit/s/Unit of Surface) is utilized.

The average *per-user capacity* (bit/s/User) is defined as

$$\bar{c} = \frac{1}{A_{\mathrm{cell}}} \iint_{\mathcal{A}_{\mathrm{cell}}} \frac{c(x,y)}{u(x,y)} dxdy, \tag{9}$$

where $\mathcal{A}_{\mathrm{cell}}$ denotes the cell region, A_{cell} the corresponding area, $c(x, y)$ (bit/s/Unit of Surface) is the capacity density, as defined in (4) and $u(x, y)$ denotes the user density.

Assuming the user density to be constant ($u(x, y) = u$), (9) can be further simplified.

Then, for the analysis of the optimization problem, the concepts of *per-user capacity* and *capacity density* (i.e., per-area capacity) are fully equivalent. In this work, the user density is therefore obviated and capacity density $\bar{c}$ (bit/s/Unit of Surface) is employed as performance metric. Cell-edge capacity ($c_{5\%}$) and peak capacity ($c_{95\%}$) also refer to per-area capacity densities $\left(\mathrm{bit/s/m^2}\right)$.

In terms of FFR, the average capacity density as a measure for the average per-user performance is formulated as:

$$\bar{c}\,(\rho, \beta_{\mathrm{FR}}) = \frac{1}{A_{\mathrm{cell}}} \left[\iint_{\mathcal{A}_{\mathrm{FR}}(\rho)} c_{\mathrm{FR},\rho,\beta_{\mathrm{FR}}}(x,y) dxdy + \iint_{\mathcal{A}_{\mathrm{PR}}(\rho)} c_{\mathrm{PR},\rho,\beta_{\mathrm{FR}}}(x,y) dxdy \right], \tag{10}$$

where $\mathcal{A}_{\mathrm{FR}}(\rho)$ and $\mathcal{A}_{\mathrm{PR}}(\rho)$ are the regions of the FR- and PR zone and $A_{\mathrm{FR}}(\rho)$ and $A_{\mathrm{PR}}(\rho)$ their corresponding areas, with $A_{\mathrm{cell}} = A_{\mathrm{FR}}(\rho) + A_{\mathrm{PR}}(\rho)$. Thus, $c_{\mathrm{FR},\rho,\beta_{\mathrm{FR}}}(x, y)$ and $c_{\mathrm{PR},\rho,\beta_{\mathrm{FR}}}(x, y)$ denote the capacity densities in the FR- and PR zone respectively, as defined in (7) and (8).

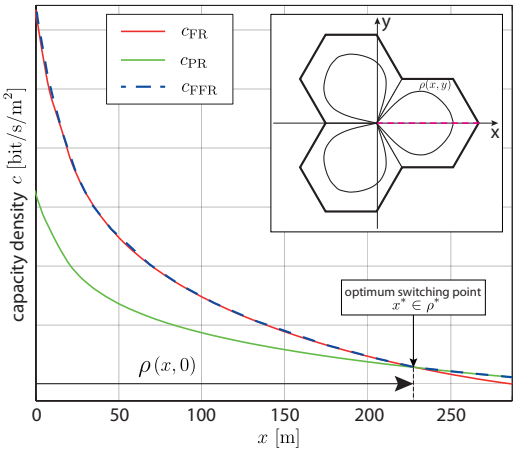

Fig. 3: Capacity densities along the center axis of a hexagonal sector. The optimum switching point, contained in ρ^*, is given by the point where $c_{\mathrm{FR}} = c_{\mathrm{PR}}$.

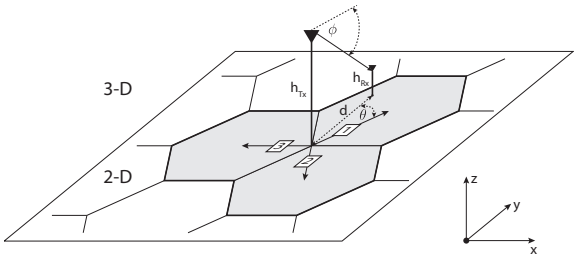

Fig. 4: 3-D sectorized scenario

IV. Optimization Proposal

To maximize the average capacity density, we allocate a user either to an FR- or PR zone, according to where the capacity density is higher:

$$c_{\mathrm{FFR},\rho,\beta_{\mathrm{FR}}}(x,y) = \max\left(c_{\mathrm{FR},\rho,\beta_{\mathrm{FR}}}(x,y), c_{\mathrm{PR},\rho,\beta_{\mathrm{FR}}}(x,y)\right). \tag{11}$$

Figure 3 illustrates the switching point for a cut of the cell. The *capacity densities* for FR (red) and PR (green) are calculated by applying (7) and (8) along the center axis of a hexagonal cell. Then, the optimal partitioning boundary (ρ^*) is calculated as

$$\rho^* = \left\{(x,y) | c_{\mathrm{FR},\rho,\beta_{\mathrm{FR}}}(x,y) = c_{\mathrm{PR},\rho,\beta_{\mathrm{FR}}}(x,y)\right\}. \tag{12}$$

In the next section, the performance of this capacity density-based FFR scheme is evaluated and compared to the FRF_1 and FRF_3 cases.

V. Simulation Results

In this setting, the cell cluster is composed of a center cell (BS_0) surrounded by six direct neighbors ($\mathrm{BS}_1 \ldots \mathrm{BS}_6$), as shown in Figure 2. The following assumptions have been made:

- Each site is equipped with three Kathrein 742 215 antennas, which are used in real network deployments [19].

TABLE I: Simulation parameters of 3-D sectorized scenario

Cell radius R [21]	250	m
Transmitter height h_{Tx}	20	m
Receiver height h_{Rx}	1.5	m
Total bandwidth B_{TOT}	5	MHz
Center frequency f_{c}	2	GHz
Noise spectral density N_0	-174	dBm
Path loss exponent α	3.6	-
Total power P_{TOT}	20	W
Antenna downtilt (electrical)	8	°

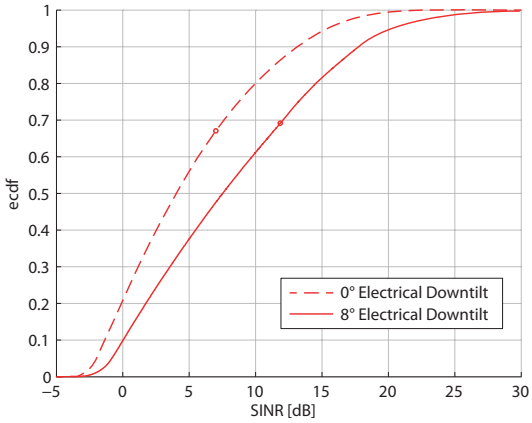

Fig. 5: SINR ECDF curves for 3-D sectorized scenario. Dots mark the average SINR.

The main radiation directions, for which an antenna gain of 18 dBi is achieved, are spaced out 120°.

- Transmitter height (h_{Tx}) and receiver height (h_{Rx}) are set to $h_{\mathrm{Tx}} = 20$ m and $h_{\mathrm{Rx}} = 1.5$ m [20], as shown in Figure 4.
- A worst-case interference situation, where all interfering Base Stations (BSs) are transmitting maximum power.
- Constant user density within the cells.

The simulation parameters are listed in Table I. Results are evaluated for the center cell (BS_0), while the surrounding cells serve as interferers. The corresponding received power densities are calculated by applying (1), where $G_{\mathrm{Tx}}(x, y)|_{\mathrm{dB}}$ is obtained from the antenna radiation pattern. In this way, the SINRs in the FR- and PR zones can be determined.

One enhancement performed in network deployments and usually not taken into account, is antenna tilting [2–5, 9, 11, 12, 14]. By tilting, the transmitted signal power is focused more strongly into the corresponding target sector and also interference in the adjacent cells is reduced. By means of it, the SINR distribution is changed, as Figure 5 shows for an example of 0° (dashed) and 8° (solid) downtilting. In literature, the simplifying assumption of noise limitation in the PR zones due to the higher FRF is usually taken [12, 14]. This setup, however, assumes interference limitation both in the PR- and FR zones.

The performance of the proposed FFR optimization method is evaluated for a case where no downtilting is applied, as well as for an 8° downtilt case.

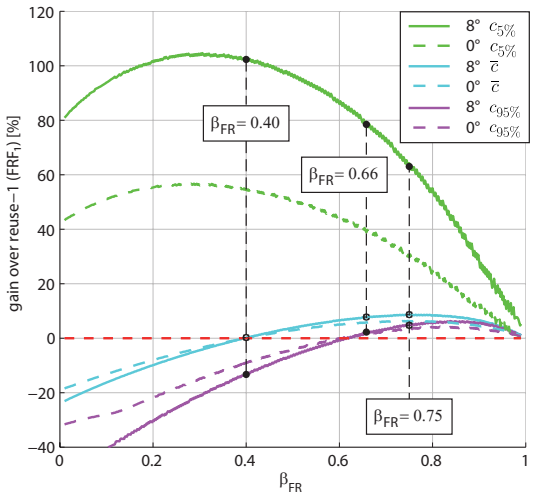

Fig. 6: Relative capacity density gains of FFR over FRF_1 scheme in 3-D sectorized scenario. Results depicted for electrically downtilting antennas by 8° (solid) and 0° (dashed), respectively.

Given the unique mapping between ρ^* and β_{FR}, as shown in (12) and Figure 3, the optimization target in (2) can be expressed as a function of solely β_{FR}, for which results are shown in Figure 6 for the non-tilted (dashed line) and downtilted (solid line) cases. The figure depicts the relative gain respective to an FRF_1 system for the average ($\bar{c}$), edge ($c_{5\%}$) and peak ($c_{95\%}$) capacity densities. In the results, we identify three relevant result sets:

- $\beta_{\mathrm{FR}} = 0.40$: No loss in average performance compared to an FRF_1 scheme.
- $\beta_{\mathrm{FR}} = 0.66$: Cell-edge performance equivalent to FRF_3 scheme.
- $\beta_{\mathrm{FR}} = 0.75$: Maximum achievable average capacity density.

It is found that the proposed FFR scheme outperforms an FRF_1 scheme in terms of average capacity density for $\beta_{\mathrm{FR}} > 0.4$. The maximum achievable gain in terms of average capacity density $\bar{c}$ will depend on how restrictive the edge performance constraint c_1 is set relative to the total bandwidth. Without the cell-edge constraint, the maximum average capacity density is achieved at $\beta_{\mathrm{FR}} = 0.75$, where, in the downtilted case, FFR outperforms the FRF_1 scheme by 8.68% in terms of average performance ($\bar{c}$), 61.81% in edge capacity ($c_{5\%}$), and 5.21% in peak capacity ($c_{95\%}$).

Thus, the proposed FFR scheme can effectively improve average, edge, and even peak performance. Results also show that, when utilizing antenna downtilting, the effect of FFR is magnified.

VI. Conclusion and Outlook

In this work, an optimized Fractional Frequency Reuse partitioning scheme based on the concept of capacity density

was proposed and evaluated by extensive simulation. The effectiveness of the proposed scheme was verified in a sectorized cell layout, using Three-dimensional antenna radiation patterns and applying electrical downtilting. Partial Reuse zones were assumed interference limited.

Compared to a conventional Reuse-1 scheme, simulation results show significant improvements in terms of average- and peak performance, while achieving a cell-edge performance comparable to a conventional Reuse-3 scheme. The gains were enhanced through antenna tilting due to the more optimal SINR distribution.

The proposed Fractional Frequency Reuse partitioning thus exploits the scarce spectral resource more efficiently than conventional Reuse-1 and Reuse-3 schemes, in terms of average-, peak- and cell-edge performance, thus improving the efficiency with which the limited amount of available bandwidth is employed.

ACKNOWLEDGMENTS

The authors would like to thank the LTE research group for continuous support and lively discussions. This work has been funded by the Christian Doppler Laboratory for Wireless Technologies for Sustainable Mobility, KATHREIN-Werke KG, and A1 Telekom Austria AG. The financial support by the Federal Ministry of Economy, Family and Youth and the National Foundation for Research, Technology and Development is gratefully acknowledged.

REFERENCES

[1] C. Lei and Y. Di, "Generalized frequency reuse schemes for OFDMA networks: Optimization and comparison," in *IEEE 71st Vehicular Technology Conference (VTC 2010-Spring)*, May 2010.

[2] M. Rahman and H. Yanikomeroglu, "Enhancing cell-edge performance: a downlink dynamic interference avoidance scheme with inter-cell coordination," *IEEE Transactions on Wireless Communications*, vol. 9, no. 4, April 2010.

[3] A. Simonsson, "Frequency reuse and intercell interference co-ordination in E-UTRA," in *IEEE 65th Vehicular Technology Conference (VTC 2007-Spring)*, April 2007.

[4] Z. Xie and B. Walke, "Frequency reuse techniques for attaining both coverage and high spectral efficiency in OFDMA cellular systems," in *IEEE Wireless Communications and Networking Conference (WCNC 2010)*, April 2010.

[5] A. Boustani, S. Khorsandi, R. Danesfahani, and N. MirMotahhary, "An efficient frequency reuse scheme by cell sectorization in OFDMA based wireless networks," in *Fourth International Conference on Computer Sciences and Convergence Information Technology (ICCIT '09)*, Nov. 2009.

[6] A. Najjar, N. Hamdi, and A. Bouallegue, "Efficient frequency reuse scheme for multi-cell OFDMA systems," in *IEEE Symposium on Computers and Communications (ISCC 2009)*, July 2009.

[7] P. Godlewski, M. Maqbool, M. Coupechoux, and J.-M. Kélif, "Analytical evaluation of various frequency reuse schemes in cellular OFDMA networks," in *Proceedings of the 3rd International Conference on Performance Evaluation Methodologies and Tools*, ser. ValueTools '08, 2008.

[8] V. Jungnickel, M. Schellmann, L. Thiele, T. Wirth, T. Haustein, O. Koch, W. Zirwas, and E. Schulz, "Interference-aware scheduling in the multiuser MIMO-OFDM downlink," *IEEE Communications Magazine*, vol. 47, no. 6, June 2009.

[9] M. Assaad, "Optimal fractional frequency reuse (FFR) in multicellular OFDMA system," in *IEEE 68th Vehicular Technology Conference (VTC 2008-Fall)*, Sept. 2008.

[10] M. Abaii, G. Auer, F. Bokhari, M. Bublin, E. Hardouin, O. Hrdlicka, G. Mange, M. Rahman, and P. Svac, "IST-4-027756 WINNER II D4.7.2 v1.0 interference avoidance concepts," Wireless World Initiative New Radio (WINNER), Tech. Rep.

[11] X. Zheng and B. Walke, "Enhanced fractional frequency reuse to increase capacity of OFDMA systems," in *3rd International Conference on New Technologies, Mobility and Security (NTMS 2009)*, Dec. 2009.

[12] B. Krasniqi, M. Wrulich, and C. Mecklenbräuker, "Network-load dependent partial frequency reuse for LTE," in *9th International Symposium on Communications and Information Technology (ISCIT 2009)*, Sept. 2009.

[13] Z. Xie and B. Walke, "Performance analysis of reuse partitioning techniques in OFDMA based cellular radio networks," in *IEEE 17th International Conference on Telecommunications (ICT)*, April 2010.

[14] A. Alsawah and I. Fijalkow, "Optimal frequency-reuse partitioning for ubiquitous coverage in cellular systems," in *15th European Signal Processing Conference (EUSIPCO)*, 2008. [Online]. Available: http://publi-etis.ensea.fr/2008/AF08a

[15] C. E. Shannon, "A mathematical theory of communication," *Bell Systems Technical Journal*, vol. 27, pp. 379–423,623–656, 1948.

[16] V. Abhayawardhana, I. Wassell, D. Crosby, M. Sellars, and M. Brown, "Comparison of empirical propagation path loss models for fixed wireless access systems," in *IEEE 61st Vehicular Technology Conference (VTC 2005-Spring)*, vol. 1, May 2005.

[17] S. Hamouda, S. Tabbane, and P. Godlewski, "Improved reuse partitioning and power control for downlink multi-cell OFDMA systems," in *Proceedings of the 2006 workshop on Broadband wireless access for ubiquitous networking*, ser. BWAN '06, 2006.

[18] S. Kiani and D. Gesbert, "Optimal and distributed scheduling for multicell capacity maximization," *IEEE Transactions on Wireless Communications*, vol. 7, no. 1, Jan. 2008.

[19] Kathrein-Werke KG, "Kathrein scala division - 742 215 65° panel antenna." [Online]. Available: http://www.kathrein-scala.com/catalog/742215.pdf

[20] 3GPP, "Evolved universal terrestrial radio access (E-UTRA); radio frequency (RF) system scenarios," 3rd Generation Partnership Project (3GPP), TS 36.942, May 2009. [Online]. Available: http://www.3gpp.org/ftp/Specs/html-info/36942.htm

[21] ——, "Evolved universal terrestrial radio access (E-UTRA); further advancements for E-UTRA physical layer aspects," 3rd Generation Partnership Project (3GPP), TS 36.814, March 2010. [Online]. Available: http://www.3gpp.org/ftp/Specs/html-info/36814.htm